Variability in Terrestrial Carbon Sinks Over Two Decades:

Part 1 – North America

C. Potter [1*], S. Klooster [2], M. Steinbach [3],

P. Tan [3], V. Kumar [3], R. Myneni [4], V. Genovese [2]

[1] NASA Ames Research Center, Moffett Field, CA

[2] California State University Monterey Bay, Seaside, CA

[3] University of Minnesota, Minneapolis, MN

4 Boston University, Boston, MA

Please return comments and other correspondence to:

[*] Corresponding author at

Email: cpotter@gaia.arc.nasa.gov

Tel. 650-604-6164; Fax. 650-604-4680

Draft Date: March 13, 2003

Submission to: *Geophysical Research Letters*

Running Title: TERRESTRIAL CARBON SINKS

Abstract. We have analyzed 17-years (1982-1998) of net carbon flux predictions from a simulation model based on satellite observations of monthly vegetation cover. The NASA-CASA model was driven by vegetation properties derived from the Advanced Very High Resolution Radiometer and radiative transfer algorithms that were developed for the Moderate Resolution Imaging Spectroradiometer (MODIS). We find that although the terrestrial ecosystem sink for atmospheric CO_2 on the North American continent has been fairly consistent at between +0.2 and +0.3 Pg C per year, high interannual variability in net ecosystem production (NEP) fluxes can be readily identified at locations across the continent. Areas of highest variability were detected along the extreme northern vegetated zones of Canada and Alaska, the northern Rocky Mountains, the central-western U.S. Great Plains and central farming region, across the southern U.S. and Mexico, and in coastal areas of the U.S. and Canada. Analysis of climate anomalies over this 17-year time period suggests that variability in precipitation and surface solar irradiance could be associated with trends in carbon sink fluxes within regions of high NEP variability.

1. Introduction

Carbon sequestration in ecosystems involves the net uptake of CO_2 from the atmosphere for persistent storage in sinks of terrestrial vegetation or soil pools. Land areas that consistently sequester carbon by growth in net ecosystem production are potentially important as future sinks for industrial CO_2 emissions. Conversely, land areas that do not consistently sequester carbon over time may be adding to already increasing atmospheric CO_2 from fossil fuel burning sources.

Efforts are underway in the U.S. and elsewhere to develop systems of carbon "credit trading," in which, for instance, industrial emitters of CO_2 may pay other entities, such as the owners of reforested land, for enhancements that result in net carbon sequestration to help mitigate the impacts of the industrial greenhouse gas emissions. Therefore, accurate estimates of how much carbon various types of ecosystems can absorb, and how variable large-scale carbon sink or sources fluxes are from year to year, will be fundamental to a successful system of carbon credit trading.

As a first approximation, lumped box models can be used to study biosphere-atmosphere exchange rates for trace gases, without regard for terrestrial vegetation types, ecological limitations, or interannual climate effects on CO_2 uptake and storage potential on land (Bolin et al., 1981). Although one can use a simple box model for order of magnitude estimates of carbon fluxes, these formulations are not sufficient for determining the spatial and temporal variability of a terrestrial carbon sink. Another modeling approach is to discretize the terrestrial biosphere into thousands of geo-referenced pixels, with detailed physiological processes in each pixel to transport CO_2 between the simulated land surface and the atmosphere, and to store carbon at the pixel location (e.g., Maisongrande et al. 1995; Kindermann et al., 1996; McGuire et al., 2001). This spatial modeling approach can consider not only actual vegetation types, but also the historical changes in land cover properties and vegetation type at each pixel location using satellite remote sensing. In addition, the effect of simultaneous plant, soil, and climate impacts can be captured in the physiological process description, which is uniquely valuable in a domain where there is still sparse distribution of long-term field study sites of these effects from which to gather NEP flux data for continental scale interpolations.

A computer model of this type based on satellite measurements of vegetation cover has been developed to simulate global ecosystem carbon cycling (Potter and Klooster, 1997 and 1998; Potter 1999). Our NASA-CASA (Carnegie Ames Stanford Approach) model is designed to estimate monthly patterns in plant carbon fixation, plant biomass, nutrient allocation, litter fall, soil nutrient mineralization, and carbon emissions from soils world-wide. This results in spatially discrete predictions of net ecosystem production (NEP) over nearly two decades. Direct input of satellite "greenness" data from the Advanced Very High Resolution Radiometer (AVHRR) sensor into the NASA-CASA model are used to estimate spatial variability in monthly net primary production (NPP), biomass accumulation, and litter fall inputs to soil carbon pools at a geographic resolution of 0.5° latitude/longitude. Global NPP of vegetation is predicted using the relationship between greenness reflectance properties and the fraction of absorption of photosynthetically active radiation (FPAR), assuming that net conversion efficiencies of PAR to plant carbon can be approximated for different ecosystems or are nearly constant across all ecosystems (Sellers et al., 1984; Running and Nemani, 1988; Goetz and Prince, 1998).

In this study, we analyze the NEP results of NASA-CASA model predictions from 1982 to 1998 to infer variability in sub-continental scale carbon fluxes and to better understand climate control patterns over terrestrial carbon sinks. The similar CASA NPP model application by Hicke et al. (2002) to North America began to address some of these issues. The scope of our study goes well beyond those of previous CASA applications, however, in that we present here the first of a three-part global biosphere analysis of variability in CO_2 sinks, starting with North America, and subsequently extending the analysis to Eurasia, South America, Africa, and Australia. Moving beyond the approach of Hicke et al. (2002), we report complete NASA-CASA model results for continental NEP (Potter et al, 2003), including predicted soil CO_2 respiration fluxes in addition to NPP estimates.

2. Global Data and Models

For this analysis, terrestrial NEP fluxes have been computed monthly (over the period 1982-1998) at a spatial resolution of 0.5° lat/lon using the NASA-CASA (Carnegie-Ames-Stanford) Biosphere model (Potter, 1999; Potter et al., 1999 and 2003). NASA-CASA is a numerical model of monthly fluxes of water, carbon, and nitrogen in terrestrial ecosystems (Figure 1). Our estimates of terrestrial NPP fluxes depend on inputs of global satellite observations for land surface properties and on gridded model drivers from interpolated weather station records (New et al., 2000) distributed across all the continental masses. Consequently, the NASA-CASA predictions of terrestrial NPP carbon fluxes are derived with no dependence whatsoever on climate index data, nor on atmospheric circulation model predictions of surface climate patterns.

Our fundamental approach to estimating net primary production (NPP) is to define optimal metabolic rates for carbon fixation processes, and to adjust these rate values using factors related to limiting effects of time-varying inputs of solar radiation, air temperature (TEMP), precipitation (PREC) (New et al., 2000), predicted soil moisture, and land cover (DeFries et al., 1994). Carbon (CO_2) fixed by vegetation as NPP is estimated in the ecosystem model according to the time-varying (monthly mean) fraction of photosynthetically active radiation (FPAR) intercepted by plant canopies and a light utilization efficiency term (e_{max}). This product is modified by stress factors for temperature (Ta) and moisture (W) that vary over time and space. The e_{max} term is set uniformly at 0.39 g C (MJ^{-1} PAR)

(Potter et al., 1993), a value that has been verified globally by comparing predicted annual NPP to more than 1900 field estimates of NPP (Figure 2). Interannual NPP fluxes from the CASA model have been reported (Behrenfeld et al., 2001) and checked for accuracy by comparison to multi-year estimates of NPP from field stations and tree rings (Malmström et al., 1997) and forest inventory reports (Hicke et al., 2002). Our NASA-CASA model has been validated against field-based measurements of NEP fluxes and carbon pool sizes at multiple locations in North America (Potter et al., 2001, Amthor et al., 2001, and Potter et al., 2003).

Our NASA-CASA model is designed to couple seasonal patterns of NPP to soil heterotropic respiration (R_h) of CO_2 from soils worldwide (Potter, 1999). First-order decay equations simulate exchanges of decomposing plant residue (metabolic and structural fractions) at the soil surface. The model also simulates surface soil organic matter (SOM) fractions that presumably vary in age and chemical composition. Turnover of active (microbial biomass and labile substrates), slow (chemically protected), and passive (physically protected) fractions of the SOM are represented. NEP can be computed as NPP minus total R_h fluxes, excluding the effects of small-scale fires and other localized disturbances or vegetation regrowth patterns on carbon fluxes (Schimel et al., 2001).

Whereas previous versions of the NASA-CASA model (Potter et al., 1993 and 1999) used a normalized difference vegetation index (NDVI) to estimate FPAR, the current model version instead relies upon canopy radiative transfer algorithms (Knyazikhin et al., 1998), which are designed to generate improved spatially varying FPAR products as inputs to carbon flux calculations. These radiative transfer algorithms, developed for the MODIS (MODerate resolution Imaging Spectroradiometer) aboard the NASA Terra platform, account for attenuation of direct and diffuse incident radiation by solving a three-dimensional formulation of the radiative transfer process in vegetation canopies. Monthly gridded composite data from spatially varying channels 1 and 2 of the Advanced Very High Resolution Radiometer (AVHRR) have been processed according to the MODIS radiative transfer algorithms and aggregated over the global land surface to 0.5^{o} grid resolution, consistent with the NASA-CASA model driver data for climate variables. To minimize cloud contamination effects, a maximum value composite algorithm was applied spatially for 0.5 degree pixel values.

3. Variability in Terrestrial Carbon Sinks

For global comparison purposes, we define the continental area for both North America (NA) as latitude zones higher than 13.5^{o} N within longitude zones from the Pacific dateline to eastern side of the Atlantic ocean. In terms of predicted annual NPP, the NA continent was estimated to vary between 6 and 7.5 Pg C (1 Pg = 10^{15} g) per year (Potter et al., 2003). These results for NA regional NPP fluxes are consistent with those reported by Schimel et al. (2001) based largely on predictions from numerous other global ecosystem models and inventories. As an example, Hicke et al. (2002) likewise estimated annual NPP for NA (north of 22^{o} N) at 6.2 Pg C per year, using higher spatial resolution (8-km) satellite inputs to the CASA vegetation model.

Continental scale NEP results from our NASA-CASA interannual simulations imply since 1982, the terrestrial NEP sink for atmospheric CO_2 in NA has been fairly consistent at between +0.2 and +0.3 Pg C per year (Figure 2; Potter et al., 2003). The exceptions were during relatively cool yearly periods like 1987, 1991-92, and 1995-96 when the NA continental NEP is predicted to be close to zero net flux of CO_2. It should be noted that the NASA-CASA model does not include sources of terrestrial carbon emitted to the atmosphere from ecosystem disturbances, such as from wild fires source fluxes of CO_2, nor from other major land use changes over decades.

The first step in this analysis of interannual variability was the conversion of all time series to monthly Z-score values, which can be used to specify the relative statistical location of each monthly value within the 17-year population distribution (e.g., all Januarys have adjusted with respect to the long-term mean January value). The numerical Z-score indicates the distance from the long-term monthly mean as the number of standard deviations above or below the mean. The main difference between the t-statistic and the Z-score is that the t-test uses a sample standard deviation, whereas the Z-score uses population standard deviation.

While our NASA-CASA model results show several consecutive multi-year periods during which the magnitudes of continental NA sinks for CO_2 were fairly constant, the predicted spatial pattern of these sink fluxes was actually quite variable from one year to the next. Areas showing the highest interannual variability on NEP fluxes were defined according to the number of anomalously low (LO) or anomalously high (HI) monthly events detected in the 17-year time series. We used an anomalous event threshold value of 1.7 standard deviations (SD) LO or HI relative to the long-term (1982-1998) NEP monthly mean value. In the use of a one-sided (LO or HI) statistical t-test, rejection of the null hypothesis means that there is no difference between the 17-yr average for the monthly NEP level and an anomalous monthly event. A SD > 1.7 represents the 95% LO confidence level for outliers in the population (Stockburger, 1998). Additionally, a threshold value of greater than three anomalous NEP-LO or NEP-HI monthly events was used to identify the areas of high interest for interannual variability, which insured that at all locations identified there would be, on average, at least one anomalous monthly event detected every five years in the time series.

An example NEP time series for a forest site (DeFries et al., 1994) in southeastern Canada illustrates a location where we can detect more than twice the number of anomalously HI versus LO monthly events. The strong seasonal signal in “raw” NEP predictions directly from the NASA-CASA model dominates the time series pattern, which is typical for the northern hemisphere carbon cycle. The Z-score transformed time series is shown below the “raw” NEP panel. Although there is not a readily evident upward or downward trend in the Z-score time series, this selected location illustrates a forest area that has been a net sink for carbon over the past two decades (Potter et al., 2003).

For our regional analysis, association patterns are reported with respect to the U.S. Department of Agriculture’s Major Land Resource Areas (MLRA; USDA, 1981). High interannual variability in NEP fluxes can be readily identified at locations across the continent that approach the maximum of 20 cumulative NEP-LO or NEP-HI monthly events in the time series (Figure 4). According the distribution of NEP-LO events (Figure 4a), the areas of highest variability are detected along the extreme northern vegetated zones of Canada and Alaska, the southern U.S. and Mexico, and the central-western U.S. Great Plains. According to the distribution of NEP-HI events (Figure 4b), the areas of highest variability are detected along the eastern and western coastal areas of the U.S. and Canada, the U. S. central farming and forest region, the northern Rocky Mountains, and interior Alaska. There is minimal overlap between the areas of highest cumulative NEP-LO versus NEP-HI monthly events in these two figures.

4. Associations with Climate Events

Association analysis can offer further insights into the types of dependencies that exist among variables within a large data set (Goodman and Kruskal,1954). Anomalously LO or anomalously HI monthly events for the main NASA-CASA model time series inputs of TEMP, PREC, SOLAR, and FPAR can be mapped in association with LO or HI monthly events for predicted NEP. As in the case of NEP, we used an anomalous event threshold value of 1.7 SD or greater from the long-term (1982-1998) climatic monthly mean value.

It is important to note that, because the NASA-CASA model has numerous non-linear functions that are used to transform the inputs variables of TEMP, PREC, SOLAR, and FPAR into predicted ecosystem NEP fluxes, a large fraction of anomalously LO or HI monthly events for NEP detected in Figure 4 may have no consistent associations with the four inputs variables, at the threshold value selected. This is not to imply that one input variable or another is not a dominant control over NEP fluxes, simply because we do not report it as such in the association counts below. To the contrary, many non-linear dependencies between model inputs and NEP predictions may fall below our threshold values of 1.7 SD, and hence we can compare the association counts among the four input variables with NEP anomalies only in a relative sense, rather than in an effort to explain all or most of the continent-wide NEP-LO and NEP-HI monthly events depicted in Figure 4. Association counts presented below should be considered representative samples of strong dependencies between NEP and at least one of the four input variables, rather than an exhaustive analysis of controls on NEP at every land location in Figure 4.

In the association counts of NEP with anomalous FPAR or SOLAR monthly events, we considered only two possible cases, LO with LO and HI with HI, since these two model inputs operate solely in NPP model calculations in a near-linear fashion to alter NEP estimates. This means that FPAR-LO or SOLAR-LO can decrease NPP (but not soil R_h) and hence potentially result in a NEP-LO monthly event (but not in a NEP-HI monthly event). The reverse effect on NPP-HI events (but not on soil R_h) can result from FPAR-HI or SOLAR-HI monthly events. In the association counts of NEP with anomalous TEMP or PREC monthly events, we instead considered all four possible cases, LO with LO, LO with HI, HI with LO, and HI with HI, since these two model inputs operate in both NPP and soil R_h model calculations to alter NEP estimates.

The most readily detectable association between model inputs events and NEP monthly events for North America was with anomalous FPAR (LO and HO combined) monthly events (Table 1), followed in decreasing order by SOLAR, PREC, and TEMP monthly events. Using the same threshold value of greater than three anomalous monthly events with SD >1.7 in the17-yr time series to identify pixels of interest, FPAR monthly anomalies were detected to co-occur with NEP monthly anomalies at about 9% of all the areas shown in Figure 4, whereas SOLAR monthly anomalies were detected to co-occur with NEP monthly anomalies at about 5% of all the pixel areas shown in Figure 4.

FPAR-LO monthly anomalies were detected to co-occur with NEP-LO monthly anomalies mainly in central Mexico, the western U.S. Great Plains, and the Rocky Mountain range, whereas FPAR-HI monthly anomalies were detected to co-occur with NEP-HI monthly anomalies mainly in northeastern Mexico, the western U.S. Great Plains, and eastern Canada (Figure 5a). These spatial patterns suggest that NEP is most heavily influenced by FPAR anomalies in areas that are semi-arid and/or frequently cropped, both of which can respond relatively rapidly to variable rainfall patterns.

SOLAR-LO monthly anomalies were detected to co-occur with NEP-LO monthly anomalies mainly in the Rocky Mountain range and into interior Alaska, whereas SOLAR-HI monthly anomalies were detected to co-occur with NEP-HI monthly anomalies mainly along Canada's southern coastal zones (Atlantic and Pacific), the U.S. Pacific northwest, and coastal Alaska (Figure 5b). These spatial patterns suggest that NEP is most heavily influenced by SOLAR anomalies in areas that are high in elevation or in close proximity to a coastal zone, both of which are impacted by frequent cloud cover.

Another notable association was observed for PREC-HI monthly anomalies that were detected to co-occur with NEP-LO monthly anomalies (Table 1) for about 7% of all the areas shown in Figure 4. These pixels are aggregated mainly in the combined areas of northern Mexico, the southwestern U.S. rangelands, and the central-western U.S. Great Plains. This association pattern is more difficult to explain than are patterns of FPAR and SOLAR anomalies with NEP anomalies (Figure 5). One possible explanation is that PREC-HI monthly anomalies in these areas are associated with seasons of high accumulated biomass fuel that can burn rapidly when ignited by lightning strikes. A major wildfire at these locations would depress NPP and result in a NEP-LO monthly anomaly.

5. Conclusions

Our NASA-CASA model results reveal important patterns of geographic variability in NEP within major continental areas of the terrestrial biosphere. A unique advantage of combining ecosystem modeling with global satellite drivers for vegetation cover properties is to enhance the spatial resolution of sink patterns for CO_2 in the terrestrial biosphere. On the temporal scale, this AVHRR data set used to generate FPAR input to the NASA-CASA model now extends for nearly 20 years of global monthly imagery, which permits model evaluations within the context of other global long-term data sets for climate and atmospheric CO_2 levels. We have begun to identify numerous relatively small-scale patterns throughout the world where terrestrial carbon fluxes may vary between net annual sources and sinks from one year to the next. Predictions of NEP for these areas of high interannual variability will require further validation of carbon model estimates, with focus on both flux algorithm mechanisms and potential scaling errors to the regional level.

Acknowledgments. This work was supported by grants from NASA programs in Intelligent Systems and Intelligent Data Understanding, and the NASA Earth Observing System (EOS) Interdisciplinary Science Program. We thank Joseph Coughlan of NASA Ames Research Center for helpful comments on an earlier version of the manuscript.

References

Behrenfeld, M. J., J. T. Randerson, C. R. McClain, G. C. Feldma, S. Q. Los, C. I. Tucker, P. G. Falkowski, C. B. Field, R. Frouin, W. E. Esaias, D. D. Kolber, and N. H. Pollack, Biospheric primary production during an ENSO transition. *Science* 291, 2594-2597, 2001.

Bolin, B., (Ed.) Carbon Cycle Modeling. SCOPE Report No. 16. New York: John Wiley, 1981.

DeFries, R. and J. Townshend, NDVI-derived land cover classification at global scales, *Internl. J. Remote Sensing*, 15, 3567-3586, 1994

Goodman, L. A., and W. H. Kruskal, Measures of association for cross-classifications, *J. American Statistical Assoc.,* 49, 732-764, 1954

Hicke, J. A., G. P. Asner, J. T. Randerson, C. J. Tucker, S. O. Los, R. Birdsey, J. C. Jenkins, C. B. Field, and E. A. Holland. 2002. Satellite-derived increases in net primary productivity across North America, 1982-1998. Geophysical Research Letters. 29(10): 1427, doi:10.1029/2001GL013578.

Knyazikhin, Y., J. V. Martonchik, R. B. Myneni, D. J. Diner, and S. W. Running, Synergistic algorithm for estimating vegetation canopy leaf area index and fraction of absorbed photosynthetically active radiation from MODIS and MISR data, *J. Geophys. Res.*, 103, 32,257-32,276, 1998.

Los, S. O., G. J. Collatz, L. Bounoua, P. J. Sellers, and C J. Tucker, Global interannual variations in sea surface temperature and land surface vegetation, air temperature, and precipitation, *Journal of Climate*, 14:1535-1549, 2001

Malmström, C. M., M. V. Thompson. G. P. Juday, S. O. Los, J. T. Randerson, and C. B. Field, Interannual variation in global scale net primary production: Testing model estimates. *Global Biogeochem. Cycles*. 11, 367-392, 1997.

McGuire, A. D., S. Sitch, J. S. Clein, R. Dargaville, G. Esser, J. Foley, M. Heimann, F. Joos, J. Kaplan, D. W. Kicklighter, R. A. Meier, J. M. Melillo, B. Moore III, I. C. Prentice, N. Ramankutty, T. Reichenau, A. Schloss, H. Tian, L. J. Williams, and U. Wittenberg. Carbon balance of the terrestrial biosphere in the twentieth century: Analyses of CO_2, climate and land-use effects with four process-based ecosystem models. *Global Biogeochem. Cycles*, 15, 183-206, 2001.

Melillo J. M., A. D. McGuire, D. W. Kicklighter, B. Moore III, C. J. Vorosmarty, and A. L. Schloss, Global climate change and terrestrial net primary production, *Nature*, 363, 234-240, 1993.

Myneni, R. B., C. J. Tucker, G. Asrar, and C. D. Keeling, Interannual variations in satellite-sensed vegetation index data from 1981 to 1991, *J. Geophys. Res.*, 103, 6145-6160, 1998.

New, M., M. Hulme, and P. Jones, Representing twentieth century space-time climate variability. II. Development of 1901-1996 monthly grids of terrestrial surface climate, *J. Climate* , 13, 2217-2238, 2000.

Potter, C. S., Terrestrial biomass and the effects of deforestation on the global carbon cycle. *BioScience*, 49, 769-778, 1999.

Potter, C. S., S. A, Klooster, R. B. Myneni, V. Genovese, P.-N. Tan, and V. Kumar. Continental scale comparisons of terrestrial carbon sinks estimated from satellite data and ecosystem modeling 1982-1998, *Global and Planetary Change*, (In Press), 2003.

Potter, C. S., V. Brooks-Genovese, S. A. Klooster, M. Bobo, and A. Torregrosa, Biomass burning losses of carbon estimated from ecosystem modeling and satellite data analysis for the Brazilian Amazon region. *Atmos. Environ.,* 35, 1773-1781, 2001.

Potter, C. S., S. Klooster, C. R. de Carvalho, V. Brooks-Genovese, A. Torregrosa, J. Dungan, M. Bobo, and J. Coughlan, Modeling seasonal and interannual variability in ecosystem carbon cycling for the Brazilian Amazon region. *J. Geophys. Res.* 106: 10,423-10,446, 2001.

Potter, C. S., J. Bubier, P. Crill, and P. LaFleur. Ecosystem modeling of methane and carbon dioxide fluxes for boreal forest sites. *Canadian J. Forest Research*. 31: 208–223, 2001.

Potter, C. S., S. A. Klooster, and V. Brooks, Interannual variability in terrestrial net primary production: Exploration of trends and controls on regional to global scales, *Ecosystems,* 2, 36-48, 1999.

Potter, C. S., J. T. Randerson, C. B. Field, P. A. Matson, P. M. Vitousek, H. A. Mooney, and S. A. Klooster, Terrestrial ecosystem production: A process model based on global satellite and surface data, *Global Biogeochem, Cycles*., 7, 811-841, 1993.

Schimel D, House J, Hibbard K, Bousquet P, Ciais P, Peylin P, Apps M, Baker D, Bondeau A, Brasswell R, Canadell J, Churkina G, Cramer W, Denning S, Field C, Friedlingstein P, Goodale C, Heimann M, Houghton RA, Melillo J, Moore III B, Murdiyarso D, Noble I, Pacala S, Prentice C, Raupach M, Rayner P, Scholes B, Steffen W, Wirth C, Recent patterns and mechanisms of carbon exchange by terrestrial ecosystems, *Nature*, 414:169-172, 2001.

Stockburger, D. W. Introductory Statistics: Concepts, Models, And Applications, WWW Version 1.0, http://www.psychstat.smsu.edu/sbk00.htm, 1998,

Tong, H., Nonlinear time series: a dynamical system approach. Oxford Univ. Press., 1990.

U.S. Department of Agriculture (USDA) Soil Conservation Service, Land Resource Regions and Major Land Resource Areas of the United States, USDA Agricultural Handbook No. 296, 156 p., 1981.

Vukicevic, T., B. H. Braswell, and D. Schimel, diagnostic study of temperature controls on global terrestrial carbon exchange. *Tellus* , 53B, 150-170, 2001.

Table 1. Counts of 0.5° pixels in North America for co-occurrence of model inputs events with NEP monthly anomalous events.

	NEP-LO Total 8718	**NEP-HI Total 8509**
MODEL INPUTS		
TEMP-LO	111	54
TEMP-HI	79	21
PREC-LO	10	18
PREC-HI	634	102
SOLAR-LO	487	-
SOLAR-HI	-	342
FPAR-LO	935	-
FPAR-HI	-	647

Figures and Captions

Figure 1. Schematic representation of components in the NASA-CASA model. The soil profile component [I] is layered with depth into a surface ponded layer (M_0), a surface organic layer (M_1), a surface organic-mineral layer (M_2), and a subsurface mineral layer (M_3), showing typical levels of soil water content (shaded) in three general vegetation types. The production and decomposition component [II] shows separate pools for carbon cycling among pools of leaf litter, root litter, woody detritus, microbes, and soil organic matter. Microbial respiration rate is controlled by temperature (TEMP) and litter quality (*q*).

Figure 2. NASA-CASA results from interannual simulations of NEP for North America. (a) monthly predictions, (b) 12 month running mean.

Figure 3. Time series example (1982-1999) of NEP raw values (top panel) and Z-score (bottom panel; units = SD) line plot for a temperate forest ecosystem location in southern Quebec (47° N 67° W). Units of Raw NEP are 10^2 g C m^{-2} mo^{-1}. Horizontal lines in the bottom panel mark the 1.7 SD threshold level for defining anomalously LO and HI monthly events.

Figure 4. Location of NEP monthly anomalies in the 17-yr time series (1982-1998) for (a) NEP-LO anomalies and (a) NEP-HI anomalies. Color bar shows number of LO or HI anomalous events at each pixel location.

Figure 5. Co-location of NEP monthly anomalies in the 17-yr time series (1982-1998) with (a) FPAR monthly anomalies, and (b) SOLAR monthly anomalies. Each colored pixel meets a threshold value of greater than three co-occuring events during the entire time series. Green pixels are LO-LO event

associations, Blue pixels are HI-HI event associations, and Red pixels are both LO-LO and HI-HI event associations.

Figure 1. Schematic representation of components in the NASA-CASA model.

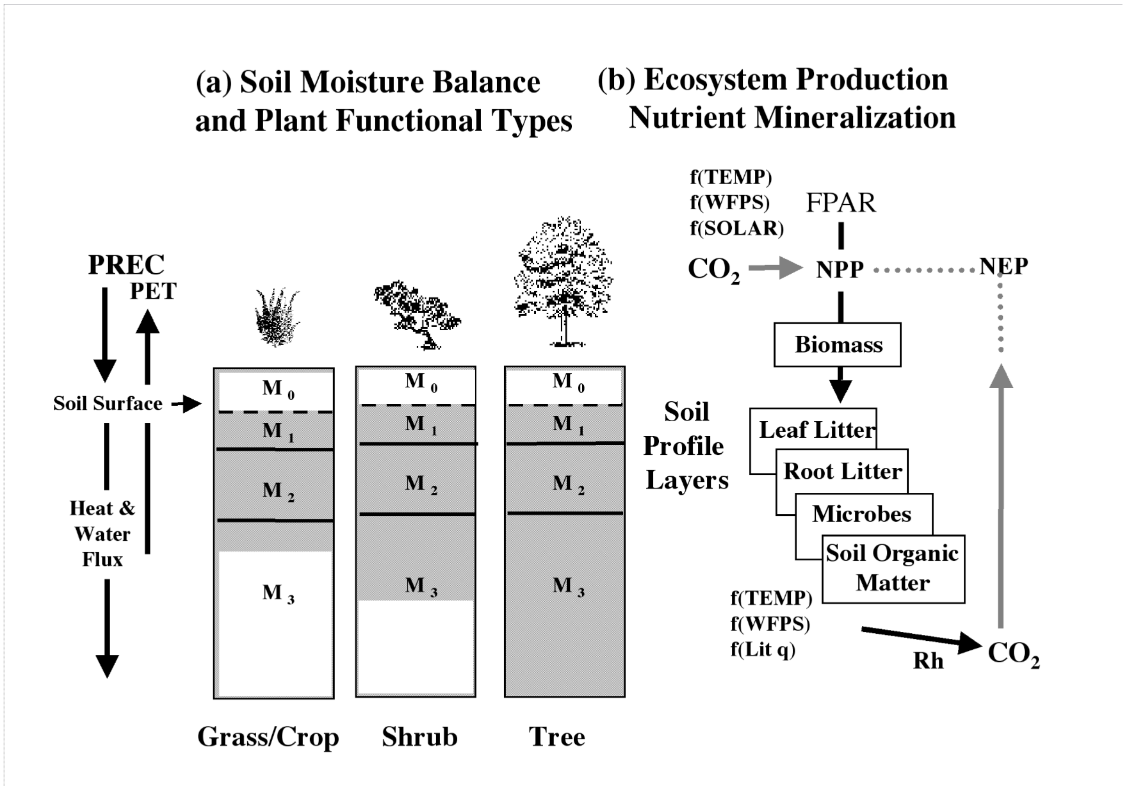

Figure 2. NASA-CASA results from interannual simulations of NEP for North America. (a) monthly predictions, (b) 12 month running mean.

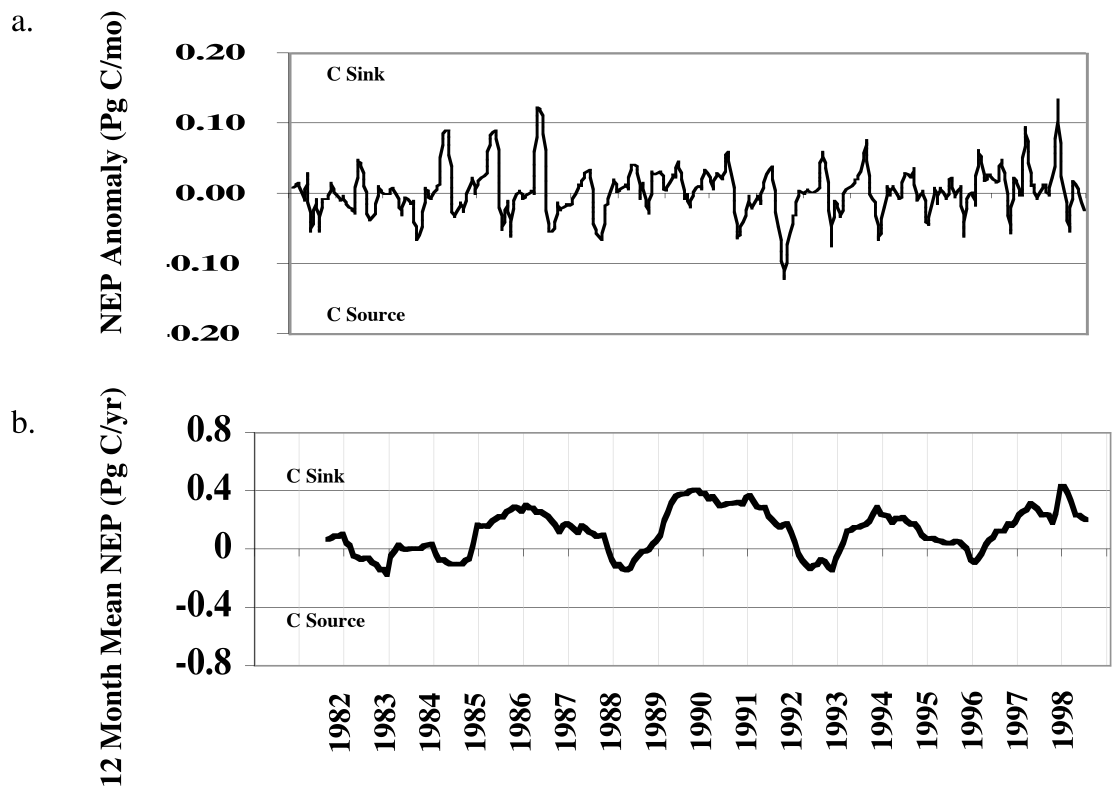

Figure 3. Time series example (1982-1999) of NEP raw values (top panel) and Z-score (bottom panel; units = SD) line plot for a temperate forest ecosystem location in southern Quebec (47° N 67° W). Units of Raw NEP are 10^2 g C m^{-2} mo^{-1}. Horizontal lines in the bottom panel mark the 1.7 SD threshold level for defining anomalously LO and HI monthly events.

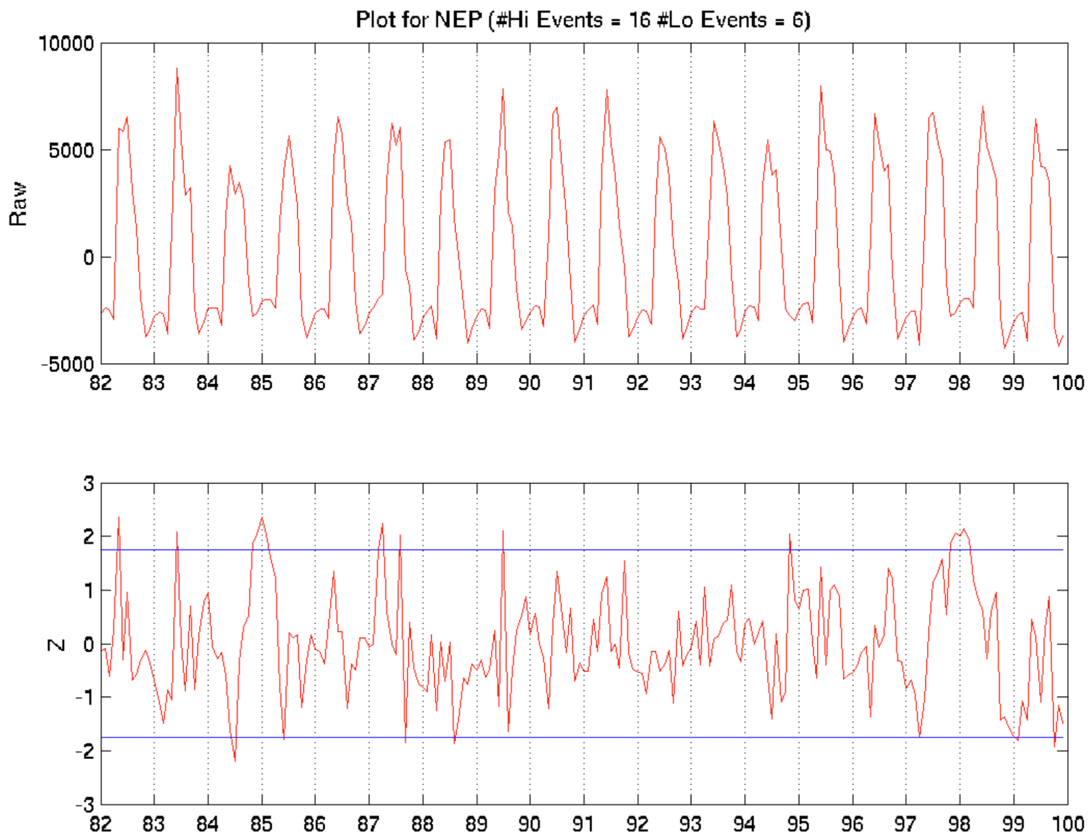

Figure 4a. NEP-LO

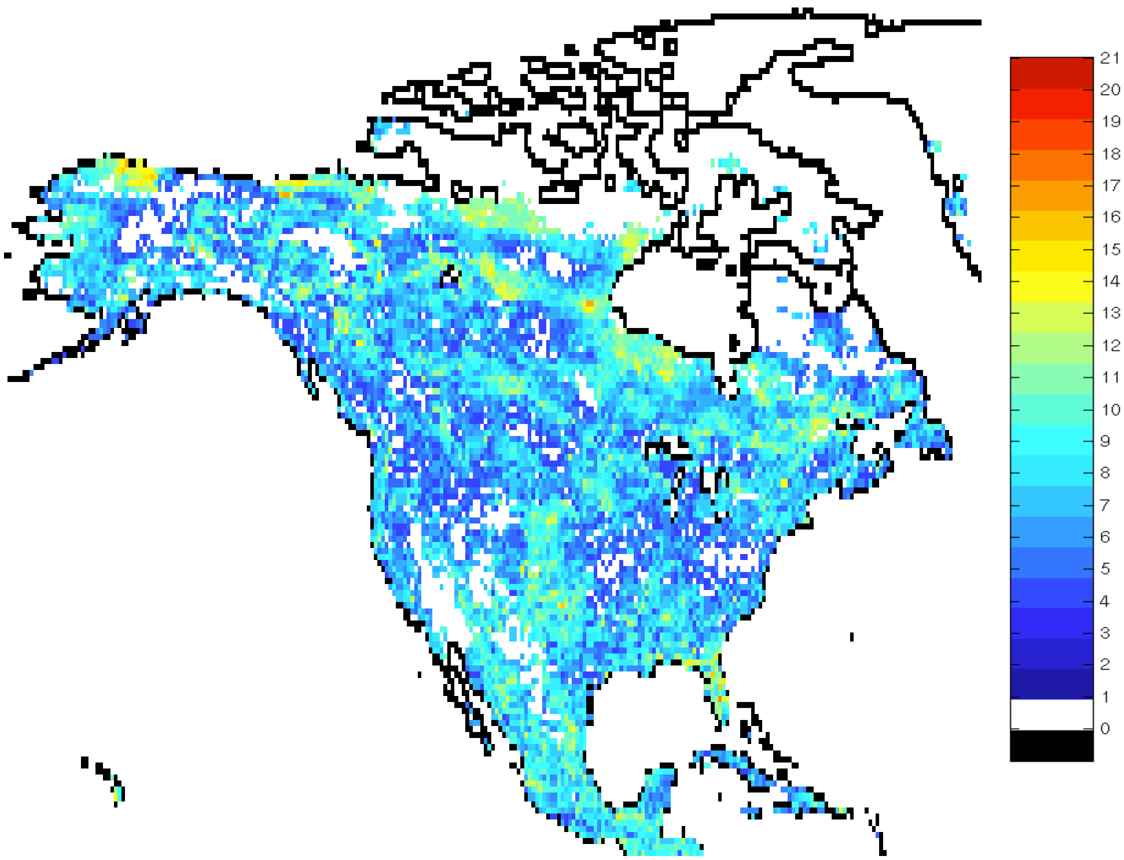

Figure 4b. NEP-HI

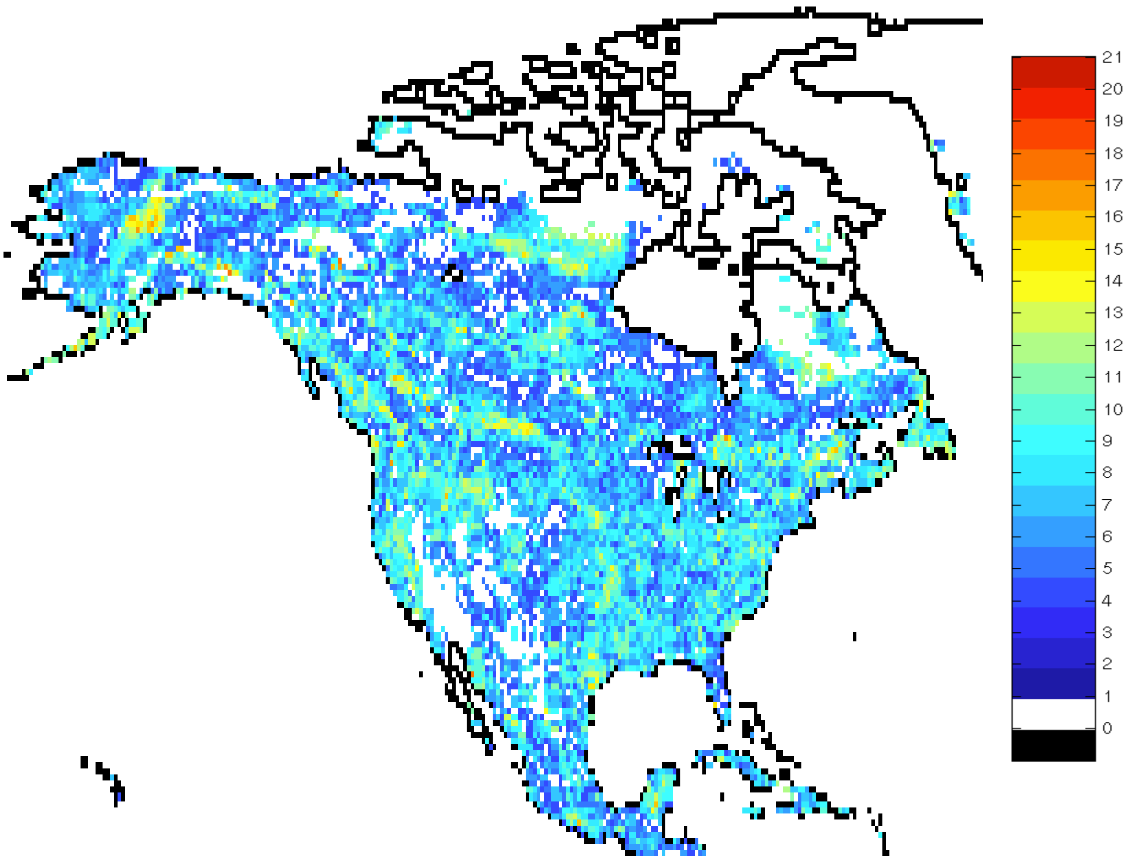

Figure 5a. Locations of FPAR with NEP monthly anomalies. Green pixels are LO-LO associations, Blue pixels are HI-HI associations, and Red pixels are both LO-LO and HI-HI associations.

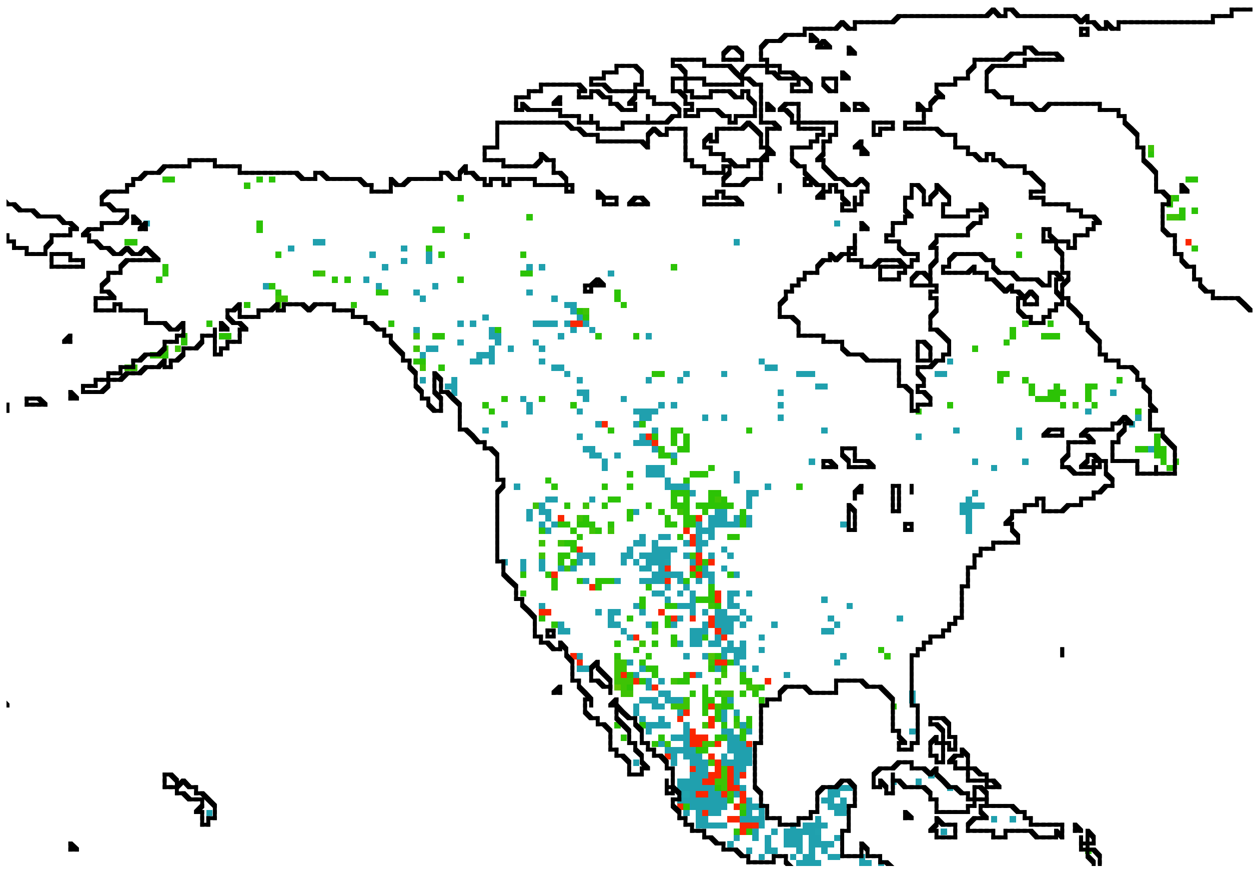

Figure 5b. Locations of SOLAR with NEP monthly anomalies. Green pixels are LO-LO associations, Blue pixels are HI-HI associations, and Red pixels are both LO-LO and HI-HI associations.